Biochimica et Biophysica Acta 1852 (2015) 893–904

Contents lists available at ScienceDirect

Biochimica et Biophysica Acta

journal homepage: www.elsevier.com/locate/bbadis

Treatment *in vitro* with PPARα and PPARγ ligands drives M1-to-M2 polarization of macrophages from *T. cruzi*-infected mice

Federico Penas [a], Gerardo A. Mirkin [a], Marcela Vera [a], Ágata Cevey [a], Cintia D. González [a], Marisa I. Gómez [a], María Elena Sales [b], Nora B. Goren [a,*]

[a] Instituto de Investigaciones en Microbiología y Parasitología Médica (IMPaM-UBA, CONICET), Buenos Aires, Argentina
[b] Centro de Estudios Farmacológicos y Botánicos (CEFyBO-UBA, CONICET), Buenos Aires, Argentina

ARTICLE INFO

Article history:
Received 26 August 2014
Received in revised form 2 December 2014
Accepted 26 December 2014
Available online 31 December 2014

Keywords:
Trypanosoma cruzi
Macrophage polarization
PPAR
Inflammatory mediators

ABSTRACT

Trypanosoma cruzi, the etiological agent of Chagas' disease, induces a persistent inflammatory response. Macrophages are a first line cell phenotype involved in the clearance of infection. Upon parasite uptake, these cells increase inflammatory mediators like NO, TNF-α, IL-1β and IL-6, leading to parasite killing. Although desired, inflammatory response perpetuation and exacerbation may lead to tissue damage. Peroxisome proliferator-activated receptors (PPARs) are ligand-dependent nuclear transcription factors that, besides regulating lipid and carbohydrate metabolism, have a significant anti-inflammatory effect. This is mediated through the interaction of the receptors with their ligands. PPARγ, one of the PPAR isoforms, has been implicated in macrophage polarization from M1, the classically activated phenotype, to M2, the alternatively activated phenotype, in different models of metabolic disorders and infection. In this study, we show for the first time that, besides PPARγ, PPARα is also involved in the *in vitro* polarization of macrophages isolated from *T. cruzi*-infected mice. Polarization was evidenced by a decrease in the expression of NOS2 and proinflammatory cytokines and the increase in M2 markers like Arginase I, Ym1, mannose receptor and TGF-β. Besides, macrophage phagocytic activity was significantly enhanced, leading to increased parasite load. We suggest that modulation of the inflammatory response by both PPARs might be due, at least in part, to a change in the profile of inflammatory macrophages. The potential use of PPAR agonists as modulators of overt inflammatory response during the course of Chagas' disease deserves further investigation.

1. Introduction

Trypanosoma cruzi (*T. cruzi*), an obligate intracellular protozoan parasite, is the etiological agent of human American trypanosomiasis, a debilitating disease widely distributed throughout Central and South America. Upon infection, the parasite has the ability to invade and multiply within diverse cell types, including macrophages. The acute phase of infection is characterized by the presence of parasites in the host bloodstream and diverse tissues. However, the heart is one of the main targets of this disease, causing serious cardiac alterations in the acute and chronic phases. A crucial step in cardiomyopathy is the infiltration of monocytes and their differentiation into macrophages. These cells may either inhibit *T. cruzi* multiplication or provide a favorable environment in which it can divide and be disseminated to other sites within the body [1].

Macrophages are a heterogeneous cell population that adapts and responds to a large variety of microenvironmental signals. They play essential roles in immunity and lipid homeostasis and, as professional scavengers, they phagocytize microbes and apoptotic and necrotic cells. Although macrophages play important roles in injury responses and tissue remodeling, it is generally considered that sustained activation of these responses may precipitate pathological states. Moreover, the activation state and functions of macrophages are profoundly affected by different cytokines and microbial products [2]. The immune phenotype of macrophages depends on various factors, including the cellular environment and the presence of various activator molecules [3]. In addition to pathogen clearance, they also regulate the resolution of inflammatory responses. These opposing or polarized activities are initiated and maintained by immunomodulatory factors such as cytokines and microbial products and manifest in distinct activation states. While Th1 cytokines, such as interferon γ (IFNγ), interleukin (IL)-1β, and lipopolysaccharide (LPS), induce a "classical" activation profile (M1), Th2 cytokines, such as IL-4 and IL-13, induce an "alternative" activation program (M2) in macrophages. Moreover, macrophages are considered plastic cells because they can switch from an activated M1

* Corresponding author at: IMPaM-UBA, CONICET, Paraguay 2155, piso 12, Buenos Aires 1121, Argentina. Tel.: +54 11 5950 9500 # 2184; fax: +54 11 4964 2554.
E-mail addresses: noragoren@hotmail.com, ngoren@fmed.uba.ar (N.B. Goren).

http://dx.doi.org/10.1016/j.bbadis.2014.12.019
0925-4439/

state back to M2, and *vice versa*, upon specific signals [4,5]. Thus, infectious or inflammatory diseases, such as chronic Chagas cardiomyopathy, may be caused not only by a sustained proinflammatory reaction but also by the failure of anti-inflammatory control mechanisms.

Peroxisome proliferator-activated receptor (PPAR)γ is a member of the nuclear hormone receptor family that has been implicated in mediating many metabolic, endocrine and cardiovascular disorders as well as inflammation [6]. Its natural ligand, 15-Deoxy-$\Delta^{12,14}$ prostaglandin J2 (15dPGJ2), has high affinity for PPARγ. Several reports have shown that 15dPGJ2 can repress some genes in activated macrophages and cardiomyocytes, including the genes for inducible nitric oxide synthase (NOS2), cyclooxygenase 2 (COX2) and tumor necrosis factor (TNF-α), and that this repression is partially dependent on PPARγ expression [7,8]. 15dPGJ2 is normally present *in vivo* during the resolution phase of inflammation, suggesting that it may function as a feedback regulator of the inflammatory response [9].

PPARα was identified in the early 1990s as a target of hypolipidemic fibrate drugs and other compounds that induce peroxisome proliferation in rodents [10]. PPARα is expressed in cells that have active fatty acid oxidation like hepatocytes, cardiomyocytes, enterocytes, smooth muscle cells, and kidney cells and has been implicated in the regulation of cellular energetic processes. PPARα ligands, such as fibrates, decrease triglyceride levels and reduce the incidence of cardiovascular events and atherosclerosis [11]. PPARα is expressed in human and mouse immune cells, including lymphocytes, macrophages, and dendritic cells, and numerous studies have implicated PPARα in the negative regulation of inflammatory responses. Different investigations using PPARα ligands have shown a reduction in the symptoms of inflammation and disease in several models, including allergic airway disease, arthritis, and inflammatory bowel disease [12].

In particular, PPARα ligands can inhibit the expression of various proinflammatory genes, such as IL-6, vascular cell adhesion molecule 1, platelet-activating factor receptor and COX2, in response to cytokine activation [13,14].

Macrophages neither appropriately suppress inflammatory cytokine production nor acquire an oxidative metabolic program associated with the M2 phenotype in the absence of PPARα signaling.

The importance of PPARγ in regulating the M1/M2 phenotypic switch has been confirmed by Amine Bouhlel et al., who demonstrated that activation of PPARγ potentiates the polarization of circulating monocytes to macrophages of the M2 phenotype [15]. Subsequent studies reported that an active PPARγ pathway is a prominent feature of alternatively activated (M2) macrophages and that M2-type responses are compromised in the absence of PPARγ expression [16]. PPARγ expression is important for the full expression of certain genes characteristic of M2 macrophages, especially the gene encoding Arginase I, a direct PPAR target [16,17]. PPARα may be involved together with PPARγ in the suppression of proinflammatory cytokines. Indeed, several studies also suggest an anti-inflammatory role for PPARα, which interferes with the NF-κB and AP-1 inflammatory pathways [18].

In the present study, we evaluated the effects of 15dPGJ2 (a natural PPARγ ligand) and WY14643 (a synthetic PPARα ligand) on the modulation of the inflammatory response and on the phenotypic changes of peritoneal macrophages from *T. cruzi*-infected mice. Also, we determined whether their polarization could modify their phagocytic functions or parasitic load.

2. Material and methods

2.1. Mice and infection

BALB/c male mice (8–10 per group) were infected intraperitoneally with 1×10^5 bloodstream trypomastigotes of a lethal RA (pantropic/reticulotropic) subpopulation of *T. cruzi* [19] and were sacrificed at 1, 2 and 6 days post infection (p.i.), depending on the experimental protocol. A 12-hour day/night cycle and water and food *ad libitum* with a standard diet were provided. Euthanasia was carried out by CO_2 inhalation. Mice used in this study were bred and maintained in the animal facility of the Department of Microbiology, Parasitology and Immunology, School of Medicine, University of Buenos Aires in accordance with the guidelines of the NIH (Guide for the Care and Use of Laboratory Animals, 1996). Protocols for animal maintenance and use were approved by the Institutional Committee for the Care and Use of Laboratory Animals (CICUAL), School of Medicine, University of Buenos Aires.

2.2. Purification of peritoneal macrophages

Macrophages were obtained by washing the peritoneal cavity of BALB/c mice with 8 ml of RPMI-1640 culture medium (Invitrogen Life Technologies, Grand Island, NY), supplemented with 10% of heat-inactivated fetal bovine serum (FBS) (Internegocios S.A., Argentina) and antibiotics (50 μg/ml of penicillin, streptomycin and gentamicin) [20]. Cells were left to adhere to the plastic surface of cell culture dishes, 35 × 10 mm (Greiner Bio One International AG) for 3 h at 37 °C under 5% CO_2 atmosphere.

2.3. In vitro treatment of macrophages with PPAR agonists

Cultured macrophages were treated with 2 μM 15dPGJ2, a PPARγ natural ligand (Sigma-Aldrich Co., St. Louis, USA) or 100 μM WY14643, a synthetic PPARα ligand (Sigma-Aldrich Co., St. Louis, USA) 3 h after cell plating. Stock 15dPGJ2 (molarity) and WY14643 (molarity) solutions were prepared in ethanol and in DMSO, respectively. Thereafter, stock solutions were diluted in culture medium to final concentrations. Treatments were performed 30 min prior to infection, when required [21]. After the different treatments cell viability was examined by a Trypan blue dye exclusion test.

2.4. FACS analysis of peritoneal exudate cells (PEC)

PEC obtained from *T. cruzi*-infected (6 dpi) and age-matched uninfected (control) mice were plated onto 24-well polystyrene plates and detached after 24 h of incubation at 37 °C under 5% CO_2. Detached cells were incubated with mAb 2.4G2 (anti-FcγR) and stained during 30 min on ice with a rat monoclonal antibody (IgG2b) to mouse F4/80, labeled with allophycocyanin (APC, AbD Serotec, Bio-Rad, USA) diluted 1:100 in FACS buffer (1× PBS containing 1% BSA and 0.1% sodium azide). Non-specific binding was controlled using an APC-labeled isotype-matched irrelevant antibody. For macrophage profiling, cells were fixed with 4% paraformaldehyde, washed with Perm-Wash™ (Becton Dickinson, USA), incubated with rabbit polyclonal antibodies to NOS2 or Arginase I at the appropriate dilution, and stained with FITC-labeled goat anti-rabbit IgG diluted in Perm-Wash™, washed twice with the same solution and resuspended in 1× PBS. At least ten thousand events were acquired using a FACSCanto flow cytometer (Becton-Dickinson, USA). The percentage of positive cells and mean fluorescence intensity (MFI) were determined using the Weasel flow cytometry software (Walter and Elisa Hall Institute, Melbourne, Australia).

2.5. NO measurement

To determine the amount of NO released into the medium, nitrate was reduced to nitrite and this was measured spectrophotometrically by the Griess reaction, as previously described [22]. The absorbance at 540 nm was compared with a standard curve of $NaNO_2$. *In situ* NO synthesis was performed in peritoneal macrophages loaded with 4-amino-5-methylamino-2′,7′-difluorofluorescein diacetate (DAF-FM), following the controls and recommendations of the supplier (Molecular Probes, Eugene, OR, USA). DAF-DM is a non-fluorescent compound

that reacts with NO to form fluorescent benzotrizole with excitation/emission at 495/515 nm [23].

2.6. Quantitative real-time reverse transcriptase-polymerase chain reaction (Q-RT-PCR)

Total RNA was extracted from frozen cells using a Trizol reagent (Life Technologies, Inc.). Total RNA was reverse transcribed using Expand Reverse Transcriptase (Invitrogen Corp.). Q-RT-PCR was performed using a 5× HOT FIREPol® EvaGreen® qPCR Mix Plus (ROX) (Solis BioDyne Corp.) in an Applied Biosystems 7500 sequence detector. Primer sequences were: TNF-α forward: 5′-ATGAGCACAGAAAGCATGATC-3′, reverse: 5′-TACAGGCTTGTCACTCGAATT-3′; IL-1β forward: 5′ TTGA CAGTGATGAGAATGACC-3′, reverse: 5′-CAAAGATGAAGGAAAAGA AGG-3′; IL-6 forward: 5′-TGATGCACTTGCAGAAAACAA-3′, reverse: 5′-GGTCTTGGTCCTTAGCCACTC-3′; PPARα forward: 5′-GCTGGTGTACGA CAAGTG-3′, reverse: 5′-GTGTGACATCCCGACAGAC-3′; PPARγ forward: 5′-ATCTACACGATGCTGGC-3′, reverse: 5′-GGATGTCCTCGATGGG-3′; NOS2 forward: 5′-CACAGCAATATAGGCTCATCCA-3′, reverse: 5′-GGAT TTCAGCCTCATGGTAAAC-3′; Ym1 forward: 5′-GGATGGCTACACTGGA GAAA-3′, reverse: 5′-AGAAGGGTCACTCAGGATAA-3′; mannose receptor (MR) forward: 5′-CAAGGAAGGTTGGCATTTGT-3′, reverse: 5′-CCTT TCAGTCCTTTGCAAGC-3′; and TGF-β forward: 5′-CACCGGAGAGCCCT GGATA-3′, reverse: TGTACAGCTGCCGCACACA-3′. All samples were analyzed in the same run for 18S expression for normalization: forward: 5′ AACACGGGAAACCTCACCC-3′ and reverse: 5′-CCACCAACTAAGAACG GCCA-3′. PCR parameters were 52 °C for 2 min, 95 °C for 15 min, and 40 cycles of 95 °C for 30 s, 63 °C (for TGF-β) or 60 °C (for NOS2, IL-6, MR, TNF-α and 18S) or 56 °C (for Ym1, IL-1β and PPARα) or 54 °C (for PPARγ) for 1 min. Quantification was calculated using the comparative threshold cycle (Ct) method and efficiency of the RT reaction (relative quantity, $2^{-\Delta\Delta Ct}$). The replicates were then averaged and fold induction was determined, considering the value at time zero as 1 [23].

2.7. Determination of cytokine levels

TNF-α, IL-1β and IL-6 were quantified in culture supernatants by enzyme-linked immunosorbent assays (ELISA) using DuoSet antibody pairs (R&D Systems, Minneapolis, MN).

2.8. Small interfering RNA (siRNA)

Macrophages were cultured up to 30–50% confluence in RPMI medium containing 5% FBS without antibiotics for 24 h. Thereafter, cells were transfected with PPARα or PPARγ siRNA that targets PPARα and PPARγ mRNA, respectively, following the manufacturer's instructions (Santa Cruz Biotechnology Inc., CA, USA). Transfections were performed with Oligofectamine (Life Technologies, Inc., CA, USA) as specified by the manufacturer. Assays for gene activity were performed at 24 and 72 h post transfection. The impact of PPARα-siRNA and PPARγ-siRNA interference on different mRNA (Section 2.6) was evaluated by Q-RT-PCR. For the assessment of the effect of RNA silencing, infections were carried out at a ratio of 5:1 parasites to a cell [23].

2.9. Preparation of cytosolic, nuclear and total protein extracts for Western blot

Cultured cells were washed with PBS and scraped off the dishes with 100 ml of buffer A (10 mmol/l HEPES; pH 7.9, 1 mmol/l EDTA, 1 mmol/l EGTA, 10 mmol/l KCl, 1 mmol/l DTT, 0.5 mmol/l phenylmethyl sulfonyl fluoride, 40 mg/ml leupeptin, 2 mg/ml tosyllysylchloromethane, 5 mmol/l NaF, 1 mmol/l $NaVO_4$, 10 mmol/l Na_2MoO_4) and NP-40 was added to reach 0.5% (vol/vol). After 15 min at 4 °C, the tubes were gently vortexed for 10 s, and cytosolic extracts were collected by centrifugation at 13,000 *g* for 30 s. The supernatants were stored at −20 °C (cytosolic extracts). Nuclear proteins were obtained by centrifugation at 13,000 *g* for 5 min, and aliquots of the supernatant (nuclear extracts) were stored at −80 °C.

Total protein extracts were obtained after washing with PBS and then lysed adding OGP (Sigma-Aldrich Co., St. Louis, USA) lysis buffer (90 ml/dish). Then, the dishes were kept on ice for 30 min with swirling and the scrapped cells were centrifuged at 7000 *g* at 4 °C for 10 min. The supernatant was transferred to a clean tube and stored at −20 °C. Protein concentration was determined by the Bradford method using a Bio-Rad Protein Assay (BIO-RAD CA., USA) reagent and bovine serum albumin (BSA) (Sigma-Aldrich Co., St. Louis, USA) as pattern protein [22]. For Western blot analysis, total proteins were boiled in Laemmli sample buffer, and equal amounts of protein (40–50 mg) were separated by 10–12% SDS-PAGE. The gels were blotted onto a Hybond-P membrane (GE Healthcare, Madrid, Spain) and incubated with the following antibodies (Abs): anti-NOS2, anti-Arginase I and anti-α-actin (Santa Cruz Biotechnology, CA, USA). The blots were revealed by enhanced chemiluminescence (ECL) in an Image Quant 300 cabinet (GE Healthcare Biosciences, PA, USA) following the manufacturer's instructions. Band intensity was analyzed using an NIH-ImageJ program [8].

2.10. Immunofluorescence and digital image analysis

Parasite staining and digital imaging were performed as previously described by Hovsepian et al., with minor modifications [23]. Briefly, macrophage cells grown on round glass coverslips were blocked with 3% normal goat serum in PBS. The percentage of infected cells and the number of amastigotes per cell were determined by analyzing the presence of intracellular amastigotes by immunofluorescence. For this purpose, a rabbit polyclonal IgG directed to *T. cruzi* and a FITC-labeled goat anti-rabbit IgG (Sigma-Aldrich Co., St. Louis, USA) were used at 1:200 dilutions (determined by titration). Macrophage cell nuclei were stained with DAPI (300 nM in PBS). At least 30 random microscopic fields (400×) and 1000 cells per culture were acquired using a Spot RT digital camera attached to an Eclipse 600 fluorescence microscope (Nikon Inc., USA). Cell quantification was performed with the ImageJ open source software developed at the NIH, USA.

2.11. Phagocytic assay

Macrophages were infected with *T. cruzi* and cultured at 37 °C and 5% CO_2 for 48 h. Then, the cultures were challenged with 50 FITC-labeled *E. coli* per cell. Phagocytosis was stopped after 60 min by washing the macrophages with ice-cold PBS. Afterwards, macrophages were incubated with 1% antibiotic (streptomycin and penicillin) for 30 min to eliminate microorganisms that were not phagocyted. The number of *E. coli* engulfed by macrophages was determined by FACS. The distinction between internalized bacteria cells and bacteria attached to the cell surface was done by quenching of extracellular FITC fluorescence with trypan blue [24]. The remaining fluorescence was quantified on a Partec PAS III flow cytometer, and the data were analyzed with WinMDI software. The uptake index was calculated multiplying the percentage of FITC-positive cells by the mean fluorescence intensity. Uninfected animals were used as controls.

2.12. Statistical analysis

Results are expressed as the mean ± SD of at least three separate experiments. *P* values were determined using Student's *t*-test. Differences were considered statistically significant when $P < 0.05$. The differences between the different test groups for the percentages of infected cells and for the number of amastigotes *per* cell were determined using one-way ANOVA and the Tukey post-test at a significance level of $\alpha = 0.05$. NO levels using DAF-FM and fluorescence microscopy were quantified by integrating the area under the curve (AUC) fluorescence (or

integrated fluorescence density distribution), under the assumption that pixel density is directly proportional to NO production. The differences were established for a significance level of $\alpha = 0.05$ by one-way ANOVA and Bonferroni post-test for multiple comparisons. Statistical analyses were performed using the GraphPad Prism 4.0 program.

3. Results

3.1. Macrophage activation in a mouse model of T. cruzi infection

Since peritoneal exudate cells are heterogeneous in composition we sought to determine the proportion of macrophages in our preparations. Flow cytometry analysis demonstrated that more than 75% of the adherent cells expressed the macrophage-specific F4/80 marker (Fig. 1A). To determine whether peritoneal macrophages were activated after *T. cruzi* infection, NOS2 expression and nitric oxide (NO) production were analyzed as two of the main modulators of inflammation. Expression of NOS2 and production of NO in the primary culture of macrophages were assessed at 1, 2 and 6 dpi. Both were detected only at 6 dpi. At this time there was a significant expression of NOS2 ($P < 0.01$) (Fig. 1B) and release of NO (51.5 ± 4 μM *vs.* 5.5 ± 1 μM; infected *vs.* uninfected cells; $P < 0.01$) (Fig. 1C). Since NOS2 appeared at 6 dpi, we tested Arginase I expression at this time point. Fig. 1D shows a higher expression in infected mice than in controls. To determine the profile of macrophages upon *T. cruzi* infection, the expression of NOS2 and Arginase I was assessed by FACS on mouse PEC.

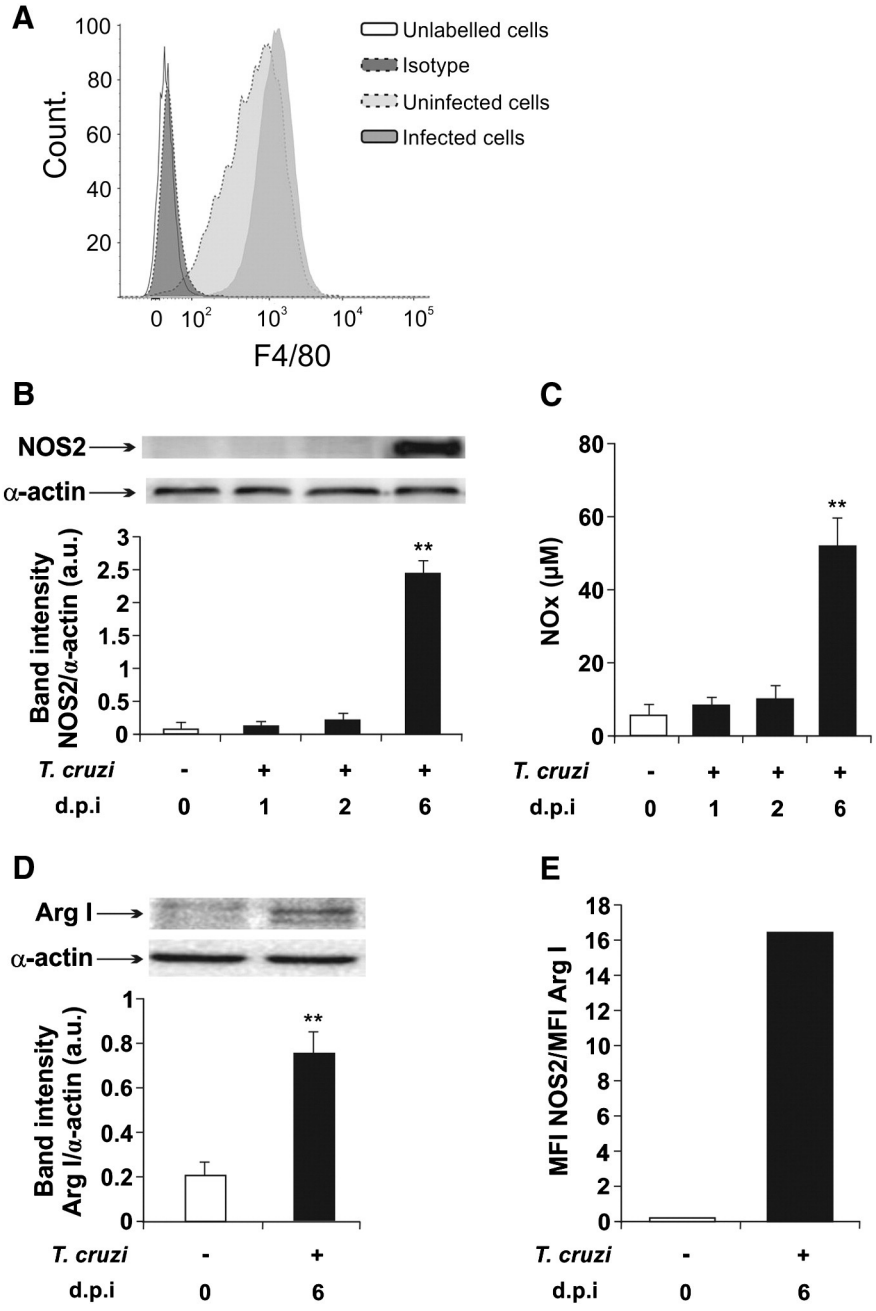

Fig. 1. Characterization of plastic-adherent peritoneal exudate cells (PECs) from *T. cruzi* infected mice. PECs were obtained from *T. cruzi*-infected and control mice. FACS analysis using an anti-F4/80 monoclonal antibody coupled to APC was used to determine the proportion of macrophages in the plastic-adherent cell fraction. A representative histogram is shown (A). Kinetics of NOS2 expression was determined by Western blot with a specific antibody. Protein levels were normalized against α-actin (B). Kinetics of NO production was quantified by a Griess reaction in the supernatants (C). Results show a representative experiment out of three performed. ** $P < 0.01$ *vs.* uninfected cells.

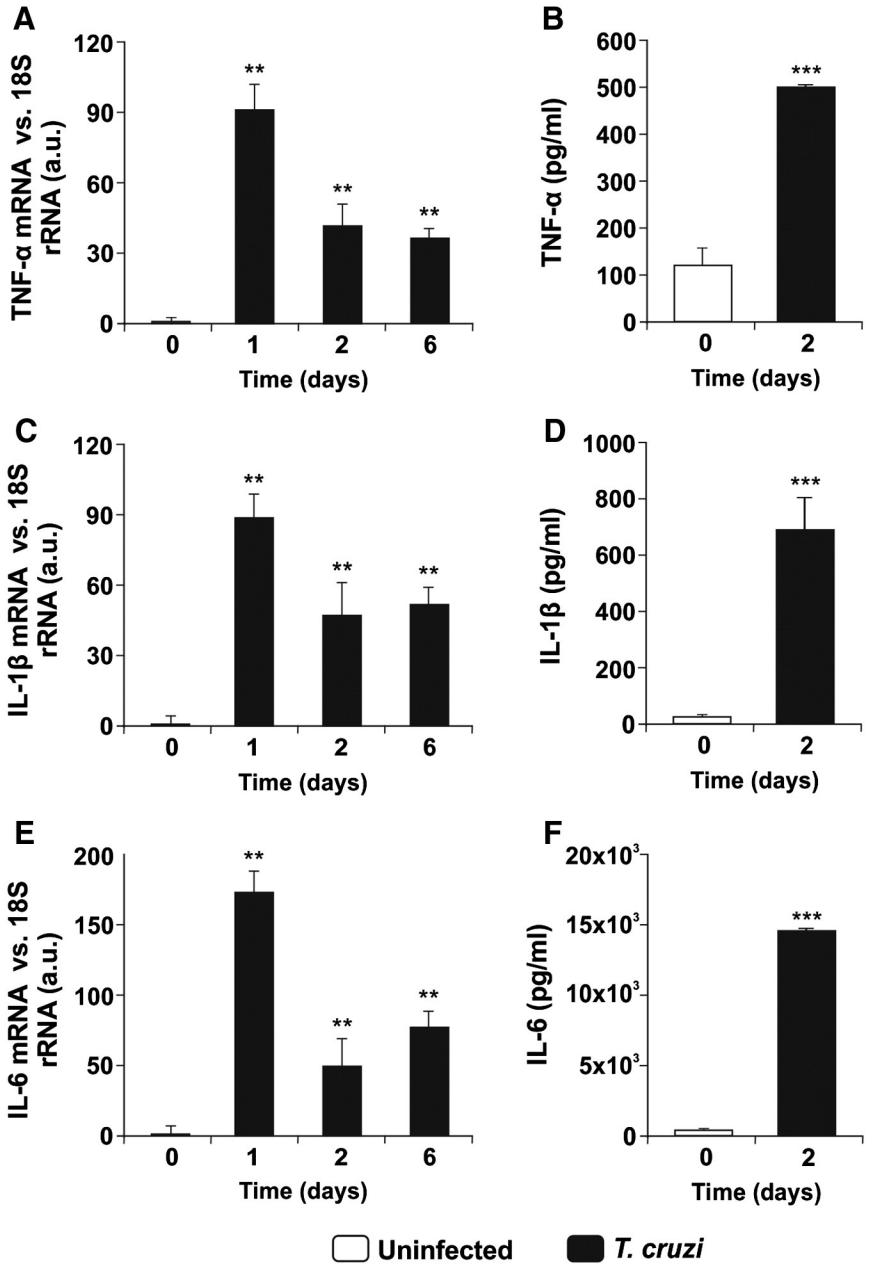

Fig. 2. Proinflammatory cytokine production by macrophages from *T. cruzi*-infected mice. Peritoneal macrophages were obtained from BALB/c mice infected with *T. cruzi*, at 1, 2 and 6 days post infection (dpi). Q-RT-PCR assays were performed and TNF-α (A), IL-1β (C) and IL-6 (E) mRNA expression was analyzed. The results were normalized against 18S rRNA. Results show a representative experiment out of three performed. ** $P < 0.01$ *vs.* uninfected cells. Quantitation of cytokine release to the culture medium was performed by capture ELISA. Bar graphs show the secretion of TNF-α (B), IL-1β (D) and IL-6 (F) by macrophages from *T. cruzi*-infected (filled bars) and control (hollow bars) mice. *** $P < 0.0001$ *vs.* uninfected cells.

Results in Fig. 1E show that the MFI ratio between NOS2 and Arginase I was higher than 1, suggesting that infection drives macrophages towards an M1 proinflammatory profile. To further confirm this, mRNA levels of proinflammatory cytokines were assessed by Q-RT-PCR. Fig. 2 shows that transcription of proinflammatory cytokine mRNA was significantly higher in macrophages from infected mice than in controls, as early as 24 h after infection. Fold induction for the different cytokines were: TNF-α (91 ± 9.1 *vs.* 1 ± 0.2, *T. cruzi vs.* uninfected, $P < 0.01$, Fig. 2A), IL-1β (88.3 ± 10 *vs.* 1 ± 0.3, *T. cruzi vs.* uninfected, $P < 0.01$, Fig. 2C) and IL-6 (174 ± 15 *vs.* 1 ± 0.2, *T. cruzi vs.* uninfected, $P < 0.01$, Fig. 2E) indicating that these macrophages are classically activated. Cytokine secretion by macrophages, 48 h after mouse infection, was measured by ELISA in culture supernatants. As shown in Fig. 2B, D and F, secretion of TNF-α, IL-1β and IL-6, respectively, was significantly higher in macrophages from *T. cruzi*-infected mice than in controls.

3.2. Macrophage M2 polarization induced by PPAR ligands

Although PPARγ ligands regulate the expression of MR, CD36 and other markers of alternative activation of macrophages [25–27], this phenomenon has not been addressed under conditions of *T. cruzi* infection. Therefore, the next step was to evaluate PPARγ and PPARα expression in macrophages from infected mice. The mRNA levels of these PPARs were significantly increased in macrophages from infected mice ($P < 0.01$ *vs.* uninfected; Fig. 3A), confirming up-regulation of these receptors under this pathological condition. No significant differences were found in the expression of PPARγ or PPARα when macrophages were treated either with 15dPGJ2 (2 μM) or WY14643 (100 μM), respectively (Fig. 3A). To determine the effects of PPAR ligands on the polarization of peritoneal macrophages, the expression of M2 macrophage activation markers was assessed by western blot and Q-RT-PCR. When

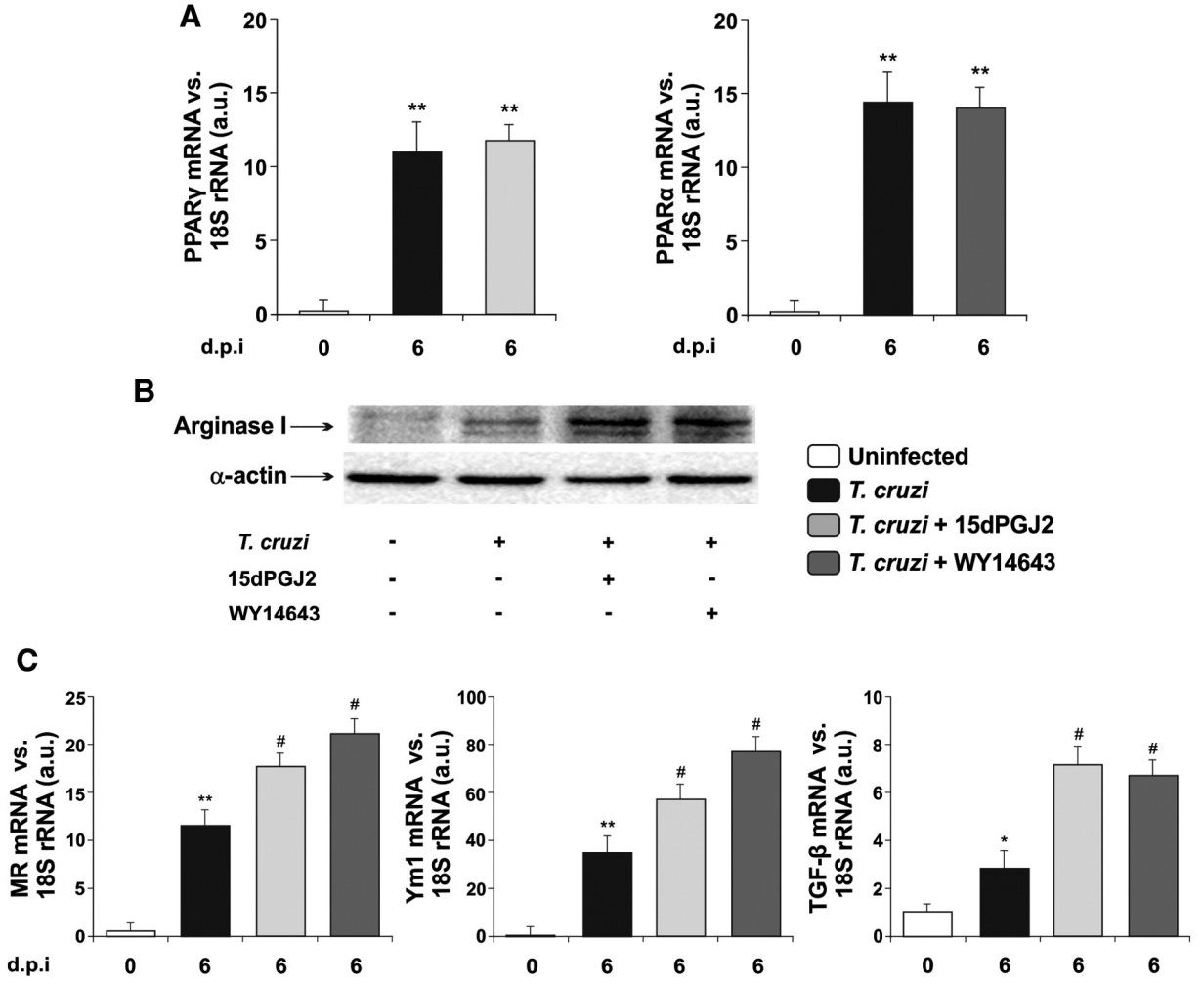

Fig. 3. Macrophage M2 polarization induced by PPAR ligands. Peritoneal macrophages were obtained from infected mice at 6 dpi and treated with 15dPGJ2 (2 μM) or WY14643 (100 μM). PPARγ and PPARα mRNA expression was analyzed by Q-RT-PCR. The results were normalized against 18S rRNA (A). Arginase I expression was determined by Western blot with a specific antibody. Protein levels were normalized against α-actin (B). MR, Ym1 and TGF-β mRNA expression was analyzed by Q-RT-PCR. The results were normalized against 18S rRNA (C). Results show a representative experiment out of three performed. * $P < 0.05$ *vs.* uninfected cells. ** $P < 0.01$ *vs.* uninfected cells. # $P < 0.05$ *vs.* untreated infected cells.

macrophages were *in vitro* treated with the PPARγ ligand 15dPGJ2 (2 μM), Arginase I protein expression increased 68.17 ± 11.6% *vs.* untreated infected cells, whereas when they were treated with the PPARα ligand WY14643 (100 μM), Arginase I protein expression increased 65.9 ± 9.8% *vs.* untreated infected cells ($P < 0.05$; Fig. 3B). In addition, MR expression increased 91.66 ± 12.9% in infected macrophages *vs.* control cells, and the treatment with 15dPGJ2 or WY14643 further increased the mRNA levels of this M2 marker (145.83 ± 17.6%; 185.83 ± 22.8%, respectively) *vs.* untreated infected cells ($P < 0.05$) (Fig. 3C). The same behavior was observed when Ym1 and TGF-β were analyzed as markers of M2 macrophages: Ym1 increased 96.99 ± 17.4% in infected cells and 15dPGJ2 and WY14643 further increased their mRNA levels (164.56 ± 13.6% and 231.53 ± 18.31%, respectively) *vs.* untreated infected cells ($P < 0.05$). The same behavior was also determined for TGF-β, which increased 64.28 ± 10.71% in infected cells in comparison to uninfected cells ($P < 0.05$) and 15dPGJ2 and WY14643 additionally increased their levels (260.71 ± 13.6% and 242.85 ± 14.24% respectively) *vs.* untreated infected cells ($P < 0.05$) (Fig. 3C). We further addressed the role of PPAR agonists with regard to macrophage polarization at the single cell level, using FACS. For this purpose, intracellular expression of NOS2 and Arginase I was determined on PPAR ligand-treated *T. cruzi*-infected and uninfected control PEC. *In vitro* treatment with PPAR agonists significantly decrease the expression of NOS2 by macrophages obtained from infected mice in comparison with untreated macrophages obtained from the same source (Fig. 4A). The same treatment significantly increases the expression of Arginase I, as shown in Fig. 4B. The NOS2/Arginase I MFI ratio significantly increased upon *T. cruzi* infection (16.3 *vs.* 0.21, infected *vs.* uninfected control), suggesting a bias towards the M1 profile. Moreover, the MFI ratios of *in vitro* PPAR ligand-treated macrophages were significantly reduced (16.3 *vs.* 3.19, infected *vs.* infected and 15dPGJ2-treated; 16.3 *vs.* 2.43, infected *vs.* infected and WY14643-treated, Fig. 4C). Treatment of PEC from uninfected mice with PPAR agonists did not induce a significant change in the expression of Arginase I or NOS2 (data not shown).

3.3. 15dPGJ2 and WY14643 inhibit NOS2, NO and pro-inflammatory cytokines

To determine whether PPARγ and PPARα modulate inflammatory mediators, infected macrophages were treated with 15dPGJ2 and WY14643, and NOS2, NO and cytokines were evaluated. Western blot assays and Q-RT-PCR also revealed that PPAR ligands are able to inhibit mRNA and NOS2 protein expression in *T. cruzi*-infected cells ($P < 0.05$ *vs.* untreated infected cells; Fig. 5A and B). In addition, we evaluated NO release by the Griess method in macrophage culture supernatants (*T. cruzi*: 53.1 ± 3.5 μM *vs.* uninfected: 5.2 ± 1 μM ($P < 0.01$); *T. cruzi* + 15dPGJ2: 28.9 ± 6.3 μM and *T. cruzi* + WY14643: 22.4 ± 5.4 μM *vs.* untreated infected cells ($P < 0.05$); Fig. 5C). These results are in agreement with *in situ* synthesis of NO by using 4-amino-5 methylamino-29,79-difluoro-fluorescein (DAF-FM), a highly sensitive

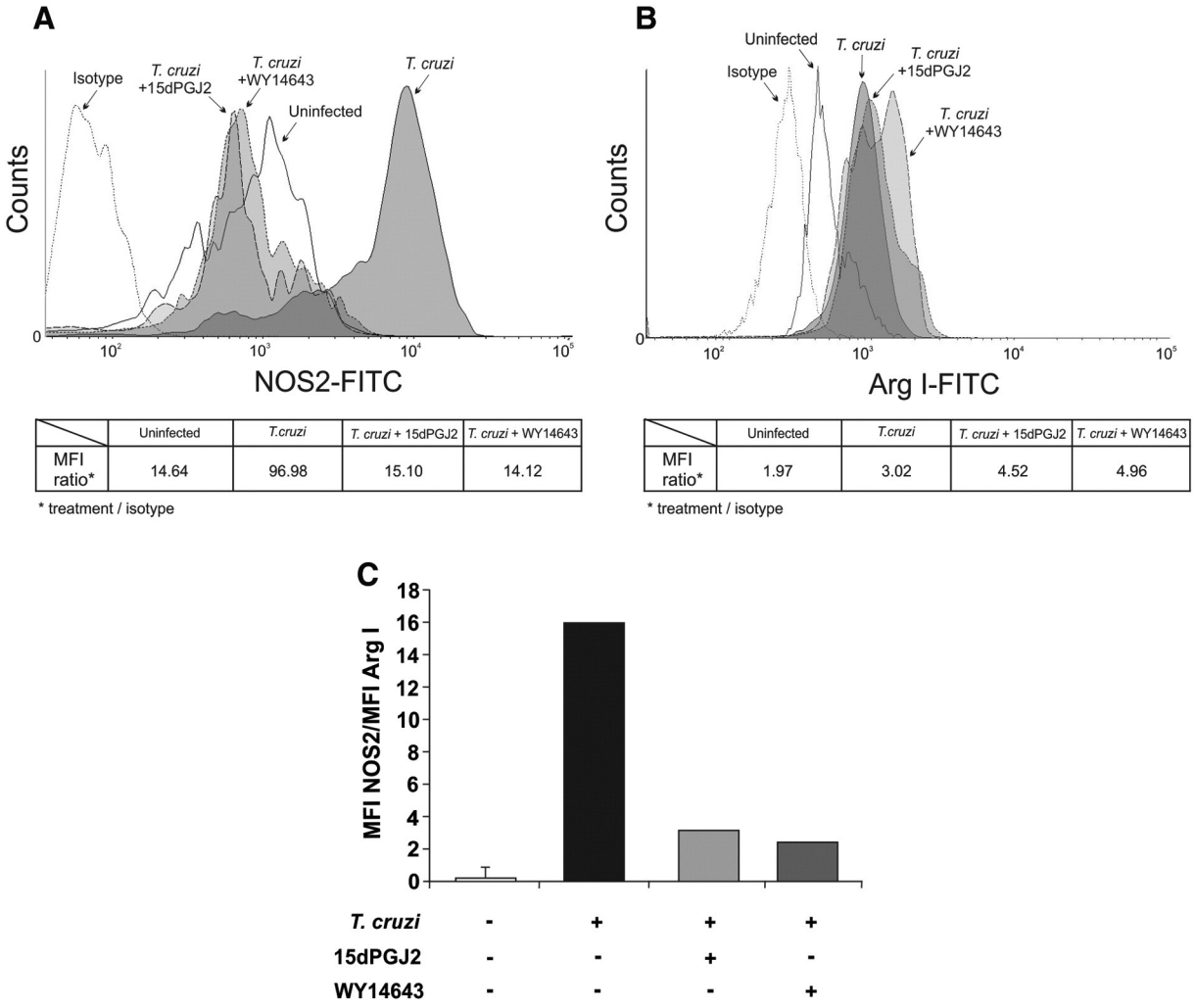

	Uninfected	T.cruzi	T. cruzi + 15dPGJ2	T. cruzi + WY14643
MFI ratio*	14.64	96.98	15.10	14.12

* treatment / isotype

	Uninfected	T.cruzi	T. cruzi + 15dPGJ2	T. cruzi + WY14643
MFI ratio*	1.97	3.02	4.52	4.96

* treatment / isotype

Fig. 4. Expression of NOS2 and Arginase I at the single cell level in PPAR ligand-treated PEC. Cells from *T. cruzi*-infected and uninfected mice were treated *in vitro* with 15dPGJ2 or WY14643. Afterwards, cells were stained for FACS according to Material and Methods. Representative histograms show the number of events and expression level of NOS2 (A) and Arginase I (B). Bar graph shows the MFI ratio of NOS2/Arginase I expression under different treatment conditions. Filled bar: PEC from infected mice, light gray: 15dPGJ2-treated PEC from infected mice, dark gray: WY14643-treated PEC from infected mice, hollow bar: PEC from uninfected mice (C).

indicator of the presence of NO. This reagent is virtually non-fluorescent until it reacts with NO, forming the fluorescent benzotriazole. After 6 days post-infection with *T. cruzi*, macrophages showed intense fluorescence, whereas those treated with 15dPGJ2 or WY14643 showed no fluorescence (Fig. 5D), indicating a clear inhibition of NO production. To assess the involvement of PPAR in these effects, PPARα and PPARγ were silenced by the corresponding siRNA, and NOS2 expression evaluated. Fig. 6 shows that when PPARα was silenced, WY14643 was unable to exert its modulator effects on NOS2 expression while 15dPGJ2 was partially able to inhibit NOS2 expression, suggesting that PPAR-independent pathways could also participate in this event. Thus, we asked whether 15dPGJ2 effects were also exerted by NF-κB, since we have previously demonstrated that this was the case for cultured primary cardiomyocytes [21]. Fig. 7 shows that the Iκ-Bα inhibitor decreased in cytosolic extracts after 30 min of infection, suggesting activation of NF-κB. Furthermore, 15dPGJ2 and WY14643 treatment inhibited Iκ Bα degradation, suggesting that PPAR ligands exert anti-inflammatory regulation through the NF-κB pathway.

When macrophages were incubated with 15dPGJ2 (2 μM) and WY14643 (100 μM), we observed a significant decrease in the mRNA expression levels of proinflammatory cytokines by Q-RT-PCR, after 24 h of infection. When TNF-α fold gene expression was evaluated, we found that *T. cruzi* increased 91 ± 9.1 *vs.* 1 ± 0.32 of the control ($P < 0.01$) and that the treatment with PPAR ligands inhibited TNF-α expression: *T. cruzi* + 15dPGJ2: 40.1 ± 12 and *T. cruzi* + WY14643: 30 ± 6.8 *vs. T. cruzi*-infected and untreated macrophages, all with $P < 0.01$ (Fig. 8A). IL-1β determination showed the following fold changes of gene expression: *T. cruzi* infection: 88.3 ± 10 *vs.* 1 ± 0.17 of the uninfected; *T. cruzi* + 15dPGJ2: 19.8 ± 3.5; and *T. cruzi* + WY14643: 31.3 ± 5.1 ($P < 0.01$) (Fig. 8C). For IL-6, we found 174 ± 15 fold of gene expression in *T. cruzi*-infected *vs.* 1 ± 0.24 of the uninfected and *T. cruzi* + 15dPGJ2 90 ± 10.3 or 90.3 ± 11 fold for *T. cruzi* + WY14643 ($P < 0.01$) (Fig. 8E). Cytokine secretion to the culture supernatant was assessed by ELISA in macrophages obtained from *T. cruzi*-infected (2 dpi) and uninfected age-matched control mice. PPARγ and PPARα agonists significantly reduced the secretion of TNF-α (Fig. 8B), IL-1β (Fig. 8D) and IL-6 (Fig. 8F) to the culture supernatants in comparison with untreated cells from infected mice. PPAR agonists didn't show a significant effect on the basal secretion of proinflammatory cytokines by macrophages from uninfected mice (data not shown).

3.4. PPAR activation enhances phagocytic activity of macrophages

To assess the phagocytic activity of infected macrophages, we performed flow cytometry assays to evaluate the internalization of *E. coli* coupled to FITC. We observed that *T. cruzi* infection increased *E. coli* internalization with an uptake index of $1 \times 10^3 \pm 120$ in comparison with $1.9 \times 10^2 \pm 23$ of the uninfected cells with $P < 0.05$ (Fig. 9A). *E. coli*

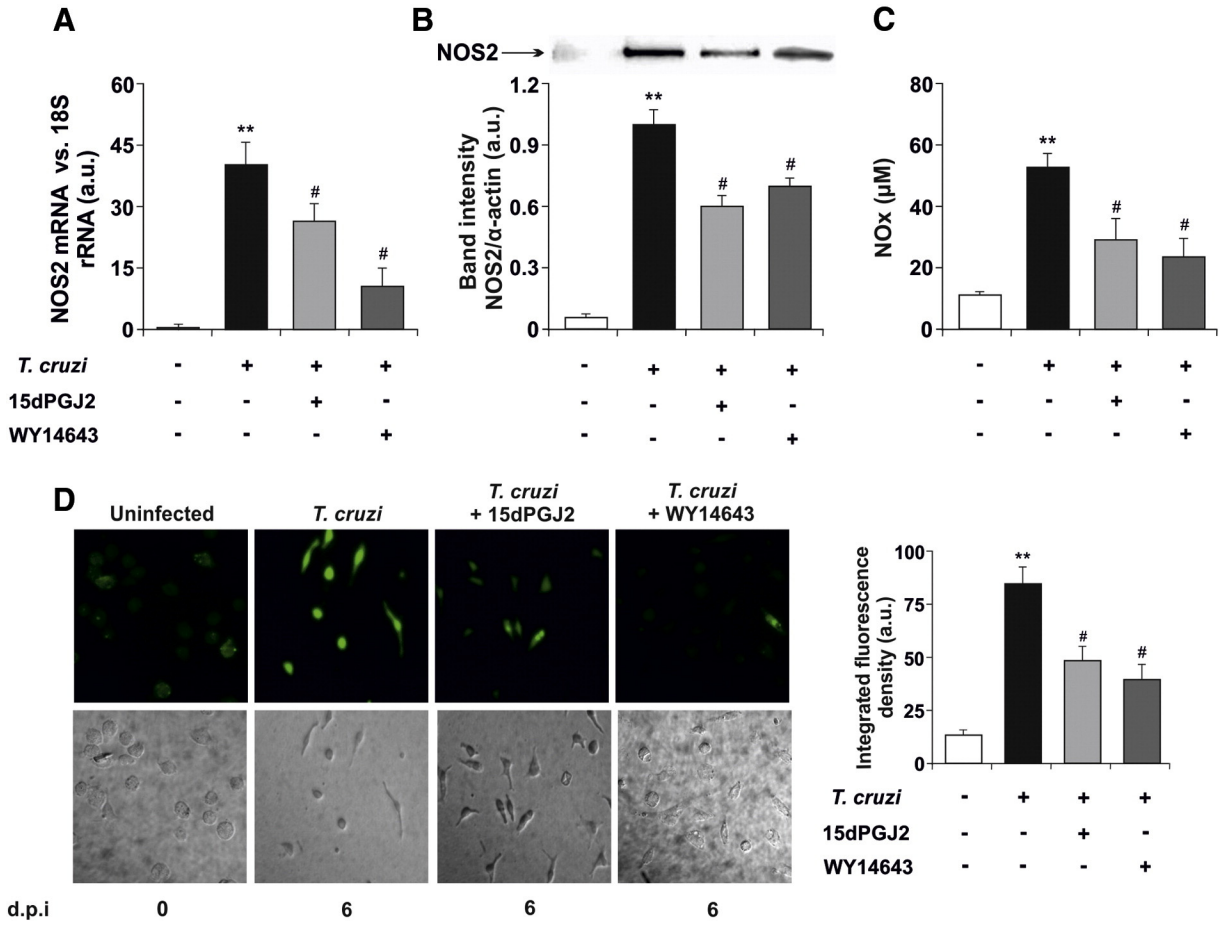

Fig. 5. 15dPGJ2 and WY14643 inhibit NOS2 expression and NO release. Peritoneal macrophages were obtained from infected mice at 6 dpi and treated with 15dPGJ2 (2 μM) or WY14643 (100 μM). NOS2 mRNA expression were analyzed by Q-RT-PCR. The results were normalized against 18S rRNA (A). NOS2 expression was determined by Western blot with a specific antibody. Protein levels were normalized against α-actin (B). NO levels were quantified by a Griess reaction in the supernatants (C). *In situ* synthesis of NO was evaluated by using the NO fluorescent probe DAF-FM and visualized by fluorescence microscopy. Microphotographs (400×) are shown. The bar graph represents the mean ± SD of the integrated fluorescence densities (D). Results show a representative experiment out of three performed. ** $P < 0.01$ *vs.* uninfected cells. # $P < 0.05$ *vs.* untreated infected cells.

internalization was enhanced by PPAR activation since the treatment with 15dPGJ2 and WY14643 increased the phagocytic activity of infected macrophages (*T. cruzi* + 15dPGJ2: $3.8 \times 10^3 \pm 250.3$; *T. cruzi* + WY14643: $5.8 \times 10^3 \pm 346.4$ uptake index with $P < 0.05$, Fig. 9B). These effects were significantly inhibited by PPARα and PPARγ silencing using siRNA, confirming that infected macrophages display enhanced phagocytic capacity, an effect amplified by PPARα and PPARγ activation ($P < 0.05$; Fig. 9B). Correspondingly, the parasite load of

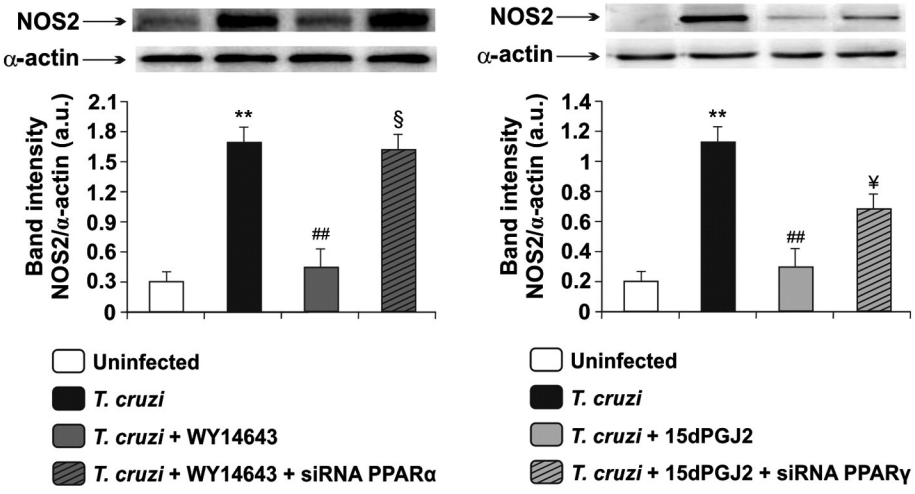

Fig. 6. PPARα and PPARγ are involved in the inhibitory effects of WY14643 or 15dPGJ2 in NOS2 expression. Peritoneal macrophages were pretreated with 15dPGJ2 (2 μM) or WY14643 (100 μM) and infected with *T. cruzi*, or transfected with PPARα or PPARγ siRNA for 72 h, treated with 15dPGJ2 (2 μM) or WY14643 (100 μM) and infected with *T. cruzi*. NOS2 expression was determined by Western blot with a specific antibody. Protein levels were normalized against α-actin. Results show a representative experiment out of three performed. ** $P < 0.01$ *vs.* uninfected cells. ## $P < 0.01$ *vs.* untreated infected cells. ¥ $P < 0.05$ *vs.* infected + 15dPGJ2 treated cells. § $P < 0.05$ *vs.* infected + WY14643 treated cells.

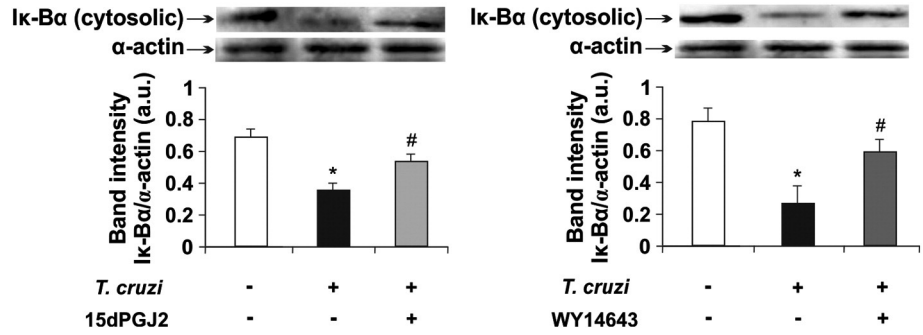

Fig. 7. Iκ-Bα expression in macrophages infected with *T. cruzi*. Macrophages pretreated or not with 15dPGJ2 (2 μM) or WY14643 (100 μM) and then infected for 30 min with *T. cruzi*. Iκ-Bα expression was determined in cytosolic extracts by Western blot with a specific antibody. Protein levels were normalized against α-actin. Results show a representative experiment out of three performed. * $P < 0.05$ *vs.* uninfected cells. # $P < 0.05$ *vs.* untreated infected cells.

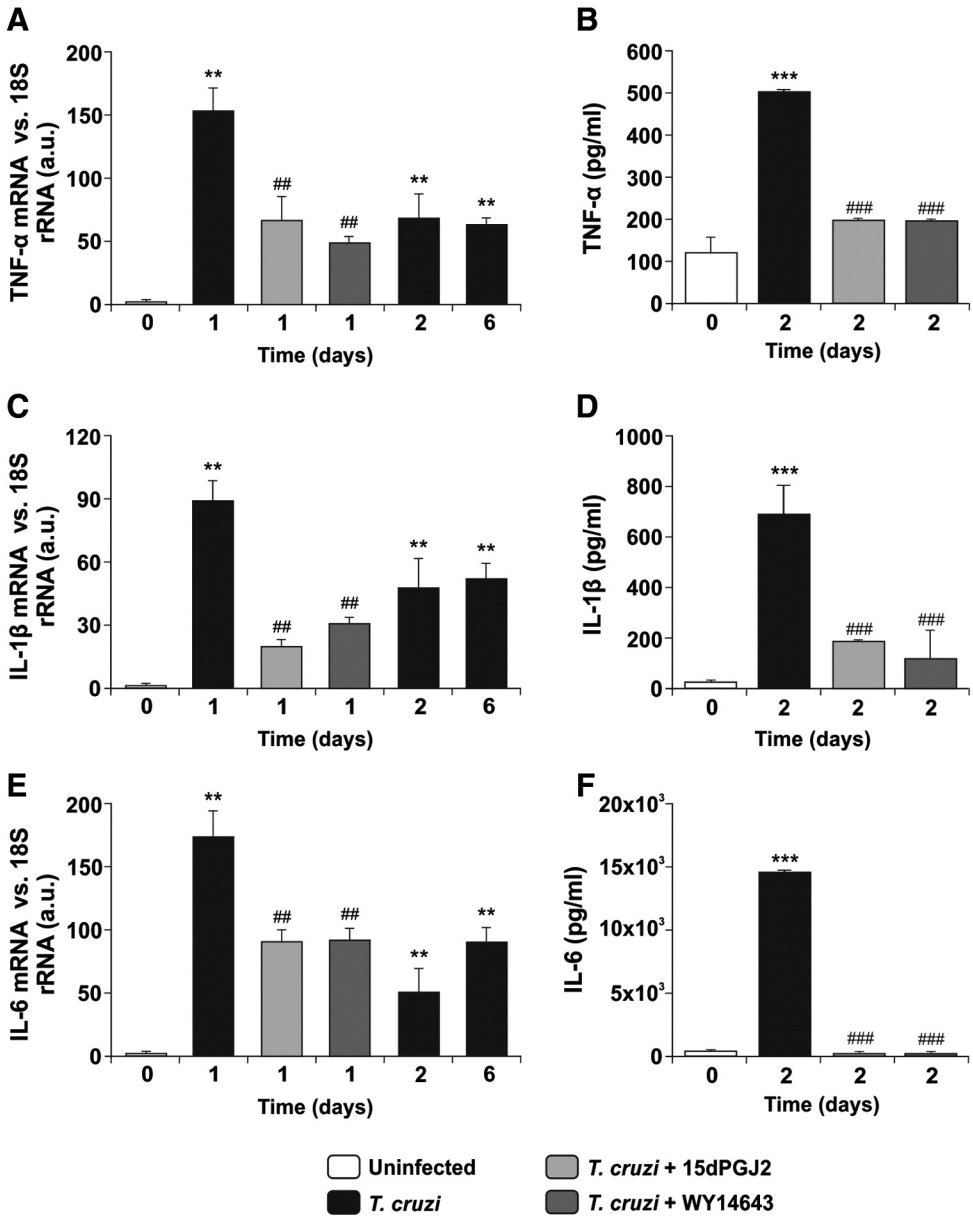

Fig. 8. Regulation of inflammatory cytokine mRNA transcription and protein secretion to culture supernatants, by 15dPGJ2 or WY14643 in macrophages from mice infected with *T. cruzi*. Peritoneal macrophages were obtained from infected mice at 1, 2 or 6 dpi and treated with 15dPGJ2 (2 μM) or WY14643 (100 μM). TNF-α (A), IL-1β (C) and IL-6 (E) mRNA expression was analyzed by Q-RT-PCR. The results were normalized against 18S rRNA. Results show a representative experiment out of three performed. ** $P < 0.01$ *vs.* uninfected cells. ## $P < 0.01$ *vs.* untreated infected cells. Quantitation of cytokine release to the culture medium was performed by capture ELISA. Bar graphs show the secretion of TNF-α (B), IL-1β (D) and IL-6 (F) of *T. cruzi*-infected (black bars), *T. cruzi*-infected 15dPGJ2-treated (light gray) and *T. cruzi*-infected WY14643-treated (dark gray) plastic adherent PECs. *** $P < 0.0001$ *vs.* uninfected cells. ### $P < 0.0001$ *vs.* untreated infected cells.

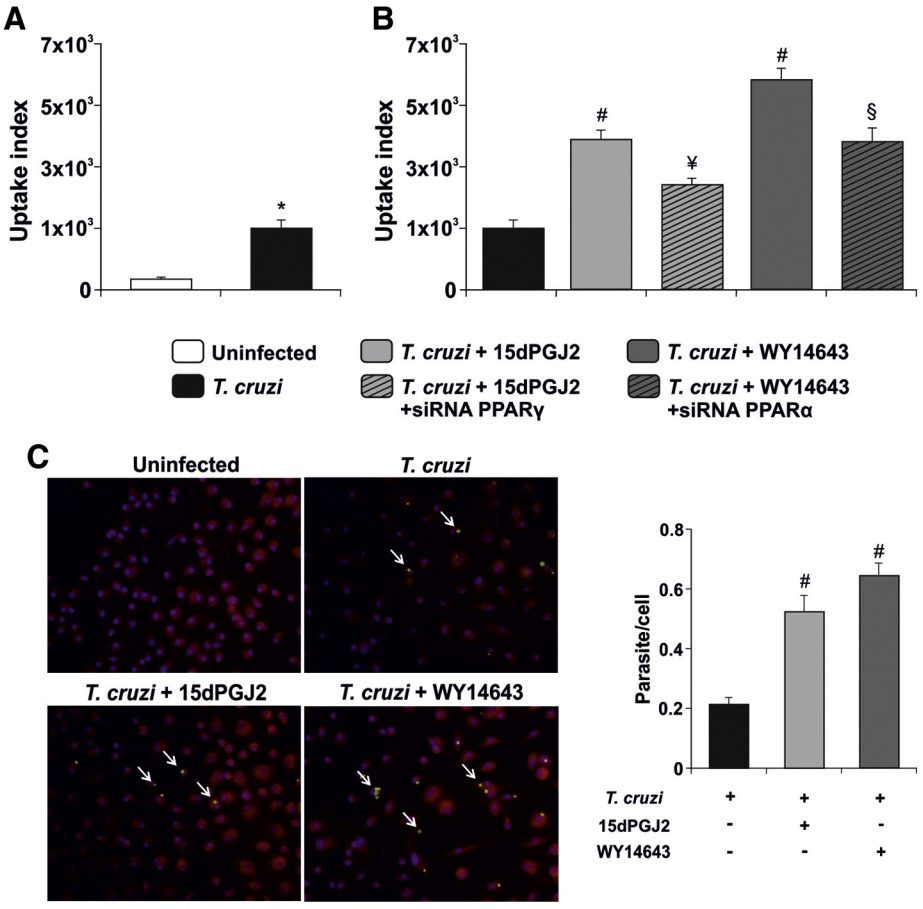

Fig. 9. Effect of 15dPGJ2 or WY14643 on the phagocytic activity and parasitism of macrophages infected with *T. cruzi*. Internalization of FITC-coupled *E. coli* by control (hollow bars) and *T. cruzi*-infected (filled bars) peritoneal macrophages was assessed by flow cytometry (A). Macrophages were pretreated with 15dPGJ2 (2 μM) or WY14643 (100 μM) and infected with *T. cruzi*, or first transfected with PPARα or PPARγ siRNA for 72 h, treated with 15dPGJ2 (2 μM) or WY14643 (100 μM) and then infected with *T. cruzi*. After 48 h, the cells were challenged with 50 FITC-labeled *E. coli* per cell and uptake was evaluated by FACS (B). Intracellular parasitism of macrophages was evaluated by fluorescence microscopy using rabbit polyclonal serum against to *T. cruzi*, followed by FITC-labeled goat anti-rabbit IgG. Afterwards, cells were counterstained with DAPI (300 nM). Microphotographs are representative of 30 fields taken at 400× magnification. White arrows show intracellular parasites (C). The number of parasites/cell (right bar graph) are shown. * $P < 0.05$ *vs.* uninfected cells. # $P < 0.05$ *vs.* untreated infected cells. ¥ $P < 0.05$ *vs.* infected + 15dPGJ2 treated cells. § $P < 0.05$ *vs.* infected + WY14643 treated cells.

in vitro treated (15dPGJ2 or WY14643) *T. cruzi*-infected macrophages was higher than in untreated *T. cruzi*-infected macrophages, as measured by fluorescence microscopy using a rabbit *T. cruzi*-specific primary antiserum followed by FITC-anti-rabbit-IgG ($P < 0.05$; Fig. 9C).

4. Discussion

Previous studies have reported that PPARγ ligands are able to modify the macrophage profile under different pathological conditions. In this study, we report for the first time that not only PPARγ, but also PPARα changes M1 peritoneal macrophages from *T. cruzi*-infected mice to express characteristic M2 markers. In addition, *in vitro* 15dPGJ2 and WY14643 treatment inhibits proinflammatory mediators and enhances the phagocytic activity of infected macrophages.

Our study shows that *T. cruzi* infection stimulates M1-type macrophage activation, since we observed expression of NOS2 and the release of high amounts of NO, plus increased mRNA transcription and secretion of TNF-α, IL-6 and IL-1β in cultured peritoneal macrophages. Accordingly, we have previously elucidated mechanistic aspects of the onset of the inflammatory response in different models of *T. cruzi* infection and in macrophages stimulated with lipopolysaccharide (LPS), where we demonstrated a significant increase in NOS2 production as well as in IL-6 and TNF-α mRNA expression in both cultured neonatal cardiomyocytes and hearts of infected mice [8,21,28].

This work focuses on the role of the natural PPARγ ligand and a synthetic PPARα ligand on the modulation of the inflammatory response and macrophage polarization in an *in vitro* experimental model of *T. cruzi* infection. The results show that infection significantly increases the levels of PPARγ and PPARα mRNA expression by macrophages compared to uninfected cells. Consistent with this, PPARγ expression increases in the spleen in a mouse model of visceral leishmaniasis [29]. Noteworthy, elevation of PPARγ was observed by Nagajyothi et al. in white adipose tissue (WAT), but not in brown adipose tissue (BAT), in a murine model of Chagas' disease. Significantly, the authors found higher levels of chemokine and cytokine mRNA transcription in BAT than in WAT. This suggests that PPARγ is involved in the downregulation of inflammation in this tissue [30].

Arginase I hydrolizes L-arginine into urea and ornithine, a precursor of L-proline and polyamines, implicated in anti-inflammatory response and tissue remodeling. Moreover, ornithine is a precursor in the pathway leading to putrescine synthesis, which promotes parasite growth [31–33]. Interestingly, Garrido et al. showed that cruzipain, the most relevant *T. cruzi* serin-protease, increases the mannose receptor turnover leading to an increase in Arginase I activity that promotes amastigote proliferation [33].

In the present work, we show that PPARγ and PPARα ligands influence Arginase I expression in PPAR ligand-treated primary culture macrophages derived from mice infected with *T. cruzi*. Interestingly, the

natural activators of PPARγ, 15dPGJ2, and the synthetic PPARα ligand, WY14643, induced Arginase I expression concomitantly with NOS2 inhibition. Previous studies have shown that expression of both PPARγ and Arginase I is induced by the Th2-derived cytokine IL-4 [34,35], providing a link between the two genes.

Gallardo-Soler et al. have described that PPARγ/δ drive macrophage activation towards a Th2 phenotype in a model of *Leishmania major* infection. These authors showed that PPARγ and PPARδ ligands induce intracellular amastigote growth in macrophages and that this effect is associated to increased Arginase I expression and activity, induced by these PPARs [17]. In the same line of evidence, Li et al. showed, in a model of lung cancer, that the synthetic PPARγ agonist pioglitazone induces Arginase I expression, and that this effect was dependent on the expression of PPARγ in the macrophages [36]. Since activation of PPARγ in macrophages leads to transcriptional repression of inflammatory genes, we determined characteristic markers of M1 and M2 macrophage polarization. Isolated mouse peritoneal macrophages exhibit an alternative M2 polarization upon the *in vitro* treatment with PPARγ and PPARα ligands. Indeed, mRNA expression of Ym1, MR and TGF-β, which are characteristic of M2 macrophage polarization [37], was greatly increased by 15dPGJ2 and WY14643 in the experimental model described herein. It must be noted, however, that there are conflicting results on the role of PPARα activation to drive macrophages towards an M2 profile. Bouhlel et al. showed that PPARα is not involved in M1-to-M2 bias, using correlation analysis of Q-RT-PCR studies on human monocyte-derived *in vitro* cultured macrophages [38]. On the contrary, Lovren et al. showed, in the context of visceral obesity-induced inflammation and cardiometabolic risk, that treatment of human monocytes with adiponectin is involved in the M1-to-M2 bias, through a priming effect dependent on PPARα, using the specific antagonist GW6471 [39].

We showed that peritoneal macrophages from *T. cruzi*-infected mice have an M1 phenotype characterized by production of high amounts of NO and increased TNF-α, IL-6 and IL-1β mRNA expression. Treatment with 15dPGJ2 and WY14643 inhibited these cytokines and NO production and induced anti-inflammatory factors characteristic of an M2 phenotype. Our results also show that NF-κB is activated in macrophages after infection and, upon 15dPGJ2 or WY14643 treatment Iκ-Bα degradation is inhibited, suggesting that these PPAR ligands exert anti-inflammatory regulation through PPAR-independent mechanisms involving the NF-κB pathway. In previous studies, we observed that 15dPGJ2 exerts anti-inflammatory effects in LPS- or *T. cruzi*-stimulated cardiac cells or in the heart of infected mice by means of PPARγ-dependent and -independent mechanisms involving transcription factors like NF-κB [8,21,28]. In this regard, several authors have also shown that both PPARγ and PPARα ligands may induce anti-inflammatory responses through inhibition of NF-κB and independently of their receptors [7,11,40]. Fernandez-Boyanapalli et al. demonstrated that a deficiency in PPARγ expression leads to delayed engulfment of apoptotic cells [41]. Also, Zhao et al. revealed that PPARγ agonist-induced upregulation of CD36 in macrophages enhances the ability of microglia to phagocytize red blood cells (*in vitro* assay) and suggested that it might help to improve hematoma resolution [42]. In this work, we showed that infection with *T. cruzi* increases the phagocytosis of FITC-labeled *E. coli* by macrophages in comparison with uninfected controls. Moreover, we found that treatment with either 15dPGJ2 or WY14643 further increases macrophage phagocytic activity. The roles of PPARα and PPARγ in this effect were confirmed by silencing these receptors with siRNA.

Our data provide new insights into the role of PPARα and PPARγ ligands in macrophage polarization. Also, by using PPARα and PPARγ silencing, we confirm our previous findings on the involvement of PPAR-independent pathways activated by PPAR ligands during *T. cruzi* infection.

In summary, we demonstrated that treatment with PPARα and PPARγ ligands drive macrophages towards an M2 profile, markedly inhibiting inflammatory mediators. Since PPAR signaling is involved in switching macrophage polarity to a tissue-repairing phenotype that might ameliorate inflammatory responses, we propose that treatment with PPAR ligands as coadjuvants of the current anti-parasitic treatments might be a new potential therapeutic approach, and may thus open new avenues to the pharmacological resolution of inflammation in Chagas' disease.

Acknowledgements

We are grateful to Mrs. María Isabel Bernal, Mr. Eduardo Alejandro Giménez and Mr. Ricardo Chung for their excellent technical assistance. We are also grateful to Diego Ojeda (MSc) and Grabriel Duette (MSc) for their assistance in the acquisition of FACS data. This work was supported by Universidad de Buenos Aires, Argentina (UBACyT 20020100100809), by Grants PICT 2007 No. 995 from Agencia Nacional de Promoción de Ciencia y Tecnología (ANPCyT) Argentina, and PIP 1424 from Consejo Nacional de Investigaciones Científicas y Técnicas (CONICET) Argentina and Fundación Alberto Roemmers.

References

[1] H.B. Tanowitz, L.V. Kirchhoff, D. Simon, S.A. Morris, L.M. Weiss, M. Wittner, Chagas' disease, Clin. Microbiol. Rev. 5 (1992) 400–419.
[2] J.A. Van Ginderachter, K. Movahedi, G. Hassanzadeh Ghassabeh, S. Meerschaut, A. Beschin, G. Raes, P. De Baetselier, Classical and alternative activation of mononuclear phagocytes: picking the best of both worlds for tumor promotion, Immunobiology 211 (2006) 487–501.
[3] S. Gordon, Alternative activation of macrophages, Nat. Rev. Immunol. 3 (2003) 23–35.
[4] F. Porcheray, S. Viaud, A.C. Rimaniol, C. Leone, B. Samah, N. Dereuddre-Bosquet, D. Dormont, G. Gras, Macrophage activation switching: an asset for the resolution of inflammation, Clin. Exp. Immunol. 142 (2005) 481–489.
[5] A. Mantovani, S.K. Biswas, M.R. Galdiero, A. Sica, M. Locati, Macrophage plasticity and polarization in tissue repair and remodelling, J. Pathol. 229 (2013) 176–185.
[6] J.M. Olefsky, C.K. Glass, Macrophages, inflammation, and insulin resistance, Annu. Rev. Physiol. 72 (2010) 219–246.
[7] D.S. Straus, G. Pascual, M. Li, J.S. Welch, M. Ricote, C.H. Hsiang, L.L. Sengchanthalangsy, G. Ghosh, C.K. Glass, 15-Deoxy-delta 12, 14-prostaglandin J2 inhibits multiple steps in the NF-kappa B signaling pathway, Proc. Natl. Acad. Sci. U. S. A. 97 (2000) 4844–4849.
[8] E. Hovsepian, F. Penas, N. Goren, 15-Deoxy-delta12,14 PGJ2 but not rosiglitazone regulates MMP-9, NOS-2 and COX-2 expression and function by PPARgamma-dependent and independent mechanisms in cardiac cells, Shock 34 (2010) 60–67.
[9] O.S. Gardner, B.J. Dewar, L.M. Graves, Activation of mitogen-activated protein kinases by peroxisome proliferator-activated receptor ligands: an example of nongenomic signaling, Mol. Pharmacol. 68 (2005) 933–941.
[10] I. Issemann, S. Green, Activation of a member of the steroid hormone receptor superfamily by peroxisome proliferators, Nature 347 (1990) 645–650.
[11] A. Castrillo, P. Tontonoz, Nuclear receptors in macrophage biology: at the crossroads of lipid metabolism and inflammation, Annu. Rev. Cell Dev. Biol. 20 (2004) 455–480.
[12] D.S. Straus, C.K. Glass, Anti-inflammatory actions of PPAR ligands: new insights on cellular and molecular mechanisms, Trends Immunol. 28 (2007) 551–558.
[13] P. Delerive, K. De Bosscher, S. Besnard, W. Vanden Berghe, J.M. Peters, F.J. Gonzalez, J.C. Fruchart, A. Tedgui, G. Haegeman, B. Staels, Peroxisome proliferator-activated receptor α negatively regulates the vascular inflammatory gene response by negative cross-talk with transcription factors NF-κB and AP-1, J. Biol. Chem. 274 (1999) 32048–32054.
[14] D. Hourton, P. Delerive, J. Stankova, B. Staels, M.J. Chapman, E. Ninio, Oxidized low-density lipoprotein and peroxisome-proliferator-activated receptor α downregulate platelet-activating-factor receptor expression in human macrophages, Biochem. J. 354 (2001) 225–232.
[15] M.A. Bouhlel, B. Derudas, E. Rigamonti, R. Dievart, J. Brozek, S. Haulon, C. Zawadzki, B. Jude, G. Torpier, N. Marx, B. Staels, G. Chinetti-Gbaguidi, PPARgamma activation primes human monocytes into alternative M2 macrophages with anti-inflammatory properties, Cell Metab. 6 (2007) 137–143.
[16] J.I. Odegaard, R.R. Ricardo-Gonzalez, M.H. Goforth, C.R. Morel, V. Subramanian, L. Mukundan, A. Red Eagle, D. Vats, F. Brombacher, A.W. Ferrante, A. Chawla, Macrophage-specific PPARgamma controls alternative activation and improves insulin resistance, Nature 447 (2007) 1116–1120.
[17] A. Gallardo-Soler, C. Gómez-Nieto, M.L. Campo, C. Marathe, P. Tontonoz, A. Castrillo, I. Corraliza, Arginase I induction by modified lipoproteins in macrophages: a peroxisome proliferator-activated receptor-gamma/delta-mediated effect that links lipid metabolism and immunity, Mol. Endocrinol. 22 (2008) 1394–1402.
[18] J.C. Fruchart, Peroxisome proliferator-activated receptor-alpha (PPAR-alpha): at the crossroads of obesity, diabetes and cardiovascular disease, Atherosclerosis 205 (2009) 1–8.
[19] G.A. Mirkin, M. Jones, O.P. Sanz, R. Rey, R.E. Sica, S.M. González Cappa, Experimental Chagas' disease: electrophysiology and cell composition of the neuromyopathic

inflammatory lesions in mice infected with a myotropic and a pantropic strain of *Trypanosoma cruzi*, Clin. Immunol. Immunopathol. 73 (1994) 69–79.
[20] E. de la Torre, E. Hovsepian, F. Penas, G. Dmytrenko, M.E. Castro, N. Goren, M.E. Sales, Macrophages derived from septic mice modulate nitric oxide synthase and angiogenic mediators in the heart, J. Cell. Physiol. 228 (2013) 1584–1593.
[21] E. Hovsepian, G.A. Mirkin, F. Penas, A. Manzano, R. Bartrons, N.B. Goren, Modulation of inflammatory response and parasitism by 15-deoxy-$\Delta^{12,14}$ prostaglandin J_2 in *Trypanosoma cruzi*-infected cardiomyocytes, Int. J. Parasitol. 41 (2011) 553–562.
[22] N. Goren, J. Cuenca, P. Martin-Sanz, L. Bosca, Attenuation of NF-kappaB signalling in rat cardiomyocytes at birth restricts the induction of inflammatory genes, Cardiovasc. Res. 64 (2004) 289–297.
[23] E. Hovsepian, F. Penas, S. Siffo, G.A. Mirkin, N. Goren, IL-10 inhibits the NF-κB and ERK/MAPK-mediated production of pro-inflammatory mediators by up-regulation of SOCS-3 in *Trypanosoma cruzi*-infected cardiomyocytes, PLoS One 8 (2013) e79445 (18).
[24] L. Lefèvre, A. Galès, D. Olagnier, J. Bernad, L. Perez, R. Burcelin, A. Valentin, J. Auwerx, B. Pipy, A. Coste, PPARγ ligands switched high fat diet-induced macrophage M2b polarization toward M2a thereby improving intestinal *Candida* elimination, PLoS One 5 (2010) e12828.
[25] A. Coste, M. Dubourdeau, M.D. Linas, S. Cassaing, J.C. Lepert, P. Balard, S. Chalmeton, J. Bernad, C. Orfila, J.P. Séguéla, B. Pipy, PPARgamma promotes mannose receptor gene expression in murine macrophages and contributes to the induction of this receptor by IL-13, Immunity 19 (2003) 329–339.
[26] A. Gales, A. Conduche, J. Bernad, L. Lefevre, D. Olagnier, M. Béraud, G. Martin-Blondel, M.D. Linas, J. Auwerx, A. Coste, B. Pipy, PPARgamma controls dectin-1 expression required for host antifungal defense against *Candida albicans*, PLoS Pathog. 6 (2010) e1000714.
[27] A. Berry, P. Balard, A. Coste, D. Olagnier, C. Lagane, H. Authier, F. Benoit-Vical, J.C. Lepert, J.P. Séguéla, J.F. Magnaval, P. Chambon, D. Metzger, B. Desvergne, W. Wahli, J. Auwerx, B. Pipy, IL-13 induces expression of CD36 in human monocytes through PPARgamma activation, Eur. J. Immunol. 37 (2007) 1642–1652.
[28] F. Penas, G.A. Mirkin, E. Hovsepian, A. Cevey, R. Caccuri, M.E. Sales, N.B. Goren, PPARγ ligand treatment inhibits cardiac inflammatory mediators induced by infection with different lethality strains of *Trypanosoma cruzi*, Biochim. Biophys. Acta 1832 (2013) 239–248.
[29] N. Adapala, M.M. Chan, Long-term use of an antiinflammatory, curcumin, suppressed type 1 immunity and exacerbated visceral leishmaniasis in a chronic experimental model, Lab. Investig. 88 (2008) 1329–1339.
[30] F. Nagajyothi, M.S. Desruisseaux, F.S. Machado, R. Upadhya, D. Zhao, G.J. Schwartz, M.M. Teixeira, C. Albanese, M.P. Lisanti, S.C. Chua Jr., L.M. Weiss, P.E. Scherer, H.B. Tanowitz, Response of adipose tissue to early infection with *Trypanosoma cruzi* (Brazil strain), J. Infect. Dis. 205 (2012) 830–840.
[31] C.G. Freire-de-Lima, D.O. Nascimento, M.B. Soares, P.T. Bozza, H.C. Castro-Faria-Neto, F.G. de Mello, G.A. DosReis, M.F. Lopes, Uptake of apoptotic cells drives the growth of a pathogenic trypanosome in macrophages, Nature 403 (2000) 199–203.
[32] C.C. Stempin, T.B. Tanos, O.A. Coso, F.M. Cerbán, Arginase induction promotes *Trypanosoma cruzi* intracellular replication in Cruzipain-treated J774 cells through the activation of multiple signaling pathways, Eur. J. Immunol. 34 (2004) 200–209.
[33] V.V. Garrido, L.R. Dulgerian, C.C. Stempin, F.M. Cerbán, The increase in mannose receptor recycling favors arginase induction and *Trypanosoma cruzi* survival in macrophages, Int. J. Biol. Sci. 7 (2011) 1257–1272.
[34] J.T. Huang, J.S. Welch, M. Ricote, C.J. Binder, T.M. Willson, C. Kelly, J.L. Witztum, C.D. Funk, D. Conrad, C.K. Glass, Interleukin-4-dependent production of PPAR-γ ligands in macrophages by 12/15-lipoxygenase, Nature 400 (1999) 378–382.
[35] I.M. Corraliza, G. Soler, K. Eichmann, M. Modolell, Arginase induction by suppressors of nitric oxide synthesis (IL-4, IL-10 and PGE2) in murine bone-marrow-derived macrophages, Biochem. Biophys. Res. Commun. 206 (1995) 667–673.
[36] A.L. Sorenson, J. Poczobutt, J. Amin, T. Joyal, T. Sullivan, J.T. Crossno Jr., M.C. Weiser-Evans, R.A. Nemenoff, Activation of PPARγ in myeloid cells promotes lung cancer progression and metastasis, PLoS One 6 (2011) e28133.
[37] F.O. Martinez, A. Sica, A. Mantovani, M. Locati, Macrophage activation and polarization, Front. Biosci. 13 (2008) 453–461.
[38] M.A. Bouhlel, J. Brozek, B. Derudas, C. Zawadzki, B. Jude, B. Staels, G. Chinetti-Gbaguidi, Unlike PPARgamma, PPARalpha or PPARbeta/delta activation does not promote human monocyte differentiation toward alternative macrophages, Biochem. Biophys. Res. Commun. 386 (2009) 459–462.
[39] F. Lovren, Y. Pan, A. Quan, P.E. Szmitko, K.K. Singh, P.C. Shukla, M. Gupta, L. Chan, M. Al-Omran, H. Teoh, S. Verma, Adiponectin primes human monocytes into alternative anti-inflammatory M2 macrophages, Am. J. Physiol. Heart Circ. Physiol. 299 (2010) 656–663.
[40] N.E. Buroker, J. Barboza, J.Y. Huang, The IkappaBalpha gene is a peroxisome proliferator activated receptor cardiac target gene, FEBS J. 276 (2009) 3247–3255.
[41] R.F. Fernandez-Boyanapalli, S.C. Frasch, K. McPhillips, R.W. Vandivier, B.L. Harry, D.W. Riches, P.M. Henson, D.L. Bratton, Impaired apoptotic cell clearance in CGD due to altered macrophage programming is reversed by phosphatidylserine-dependent production of IL-4, Blood 113 (2009) 2047–2055.
[42] X. Zhao, J. Grotta, N. Gonzales, J. Aronowski, Hematoma resolution as a therapeutic target: the role of microglia/macrophages, Stroke 40 (2009) 92–94.